

Article

Antimicrobial Potential of Biosynthesized Zinc Oxide Nanoparticles Using Banana Peel and Date Seeds Extracts

Nahed Ahmed Hussien 

Department of Biology, College of Science, Taif University, P.O. Box 11099, Taif 21944, Saudi Arabia; n.nahed@tu.edu.sa

Abstract: In the present study, zinc oxide nanoparticles (ZnONPs) were eco-friendly synthesized using banana peel (BPE) and date seed (DSE) extracts. Biosynthesis of both ZnONPs_BPE and ZnONPs_DSE was confirmed by using an ultraviolet–visible spectrophotometer (UV–VIS), then followed by their characterization using different analyses: scanning (SEM), transmission electron microscope (TEM), zeta potential analysis, X-ray diffraction (XRD), and Fourier-transform infrared (FTIR) spectroscopy. The antimicrobial potency of ZnONPs_BPE and ZnONPs_DSE was evaluated using a broth microdilution assay against pathogenic strains to determine the minimum inhibitory concentration (MIC) and minimum bactericidal concentration (MBC). UV spectra confirm the formation of ZnONPs-BPE (290 nm) and ZnONP_DSE (400 nm). TEM, SEM, and XRD revealed their hexagonal crystalline structures with nanoscale size ZnONPs_BPE (57.4 ± 13.8 nm, -9.62 mV) and ZnONPs_DSE (72.6 ± 17.1 nm, -5.69 mV). FTIR analysis demonstrated the presence of various functional groups on ZnONPs' surfaces that act as reducing, capping, and stabilizing agents. The biosynthesized ZnONPs demonstrated a good antimicrobial potential against Gram-positive (*Staphylococcus aureus* and *Bacillus subtilis*) and Gram-negative (*Escherichia coli* and *Salmonella enteritidis*) strains. Especially, ZnONPs-BPE has a higher antimicrobial effect against *Salmonella enteritidis* (MIC = 0.75 mg/mL, MBC = 1.5 mg/mL), while ZnONP_DSE has a higher effect against *Staphylococcus aureus* (MIC = 0.75 mg/mL, MBC = 3 mg/mL). The present results are consistent with previous studies that reported the antimicrobial potential of green ZnONPs through ROS induction that in turn damages microbial DNA. Consequently, the present results support the use of different biowastes in NPs' synthesis, which is a simple and sustainable way that helps with waste management and decreases environmental pollution.



Citation: Hussien, N.A. Antimicrobial Potential of Biosynthesized Zinc Oxide Nanoparticles Using Banana Peel and Date Seeds Extracts. *Sustainability* **2023**, *15*, 9048. <https://doi.org/10.3390/su15119048>

Academic Editors: Rakesh Bhaskar and Kannan Badri Narayanan

Received: 24 April 2023

Revised: 27 May 2023

Accepted: 31 May 2023

Published: 3 June 2023



Copyright: © 2023 by the author. Licensee MDPI, Basel, Switzerland. This article is an open access article distributed under the terms and conditions of the Creative Commons Attribution (CC BY) license (<https://creativecommons.org/licenses/by/4.0/>).

Keywords: ZnO nanoparticles; antibacterial; banana peel; date seed; green synthesis

1. Introduction

Nanoparticles (NPs) are very tiny particles (1–100 nm) with a large surface area in comparison to their volume. This provides NPs with unique physical, chemical, and biological properties [1,2]. There are different chemical and physical methods that are used in the synthesis of NPs, with well-controlled shape and size, and higher rates of production. The limitations of these methods are the use of toxic materials as precursors, production of large amounts of wastes, loss of energy, and high cost [3]. On the contrary, the green route of NPs' synthesis provides an eco-friendly, low-cost, sustainable, and safe way [4]. Different natural resources were used in NPs' green synthesis including microorganisms and plant extracts [5,6]. Green synthesis is mainly based on biological precursors but is also controlled by other reaction parameters such as pH, time, solvent, temperature, and pressure. Biological extracts have various effective phytochemicals such as ketones, aldehydes, phenols, flavones, terpenoids, amides, carboxylic acids, and ascorbic acids that help in metal/metal oxide NPs' synthesis [7]. Green synthesized NPs were investigated for use in antimicrobial, biomedical diagnostics, catalysis, optical imaging, molecular sensing, and the labeling of biological systems [8].

There are about 11.2 billion tons of solid waste that are generated every year according to the Environment Program of the United Nations (UNEP), 2020. Solid waste includes garbage food waste, rubber tires, construction debris, electronic waste, industrial sludges, plastics, and other discarded materials. Solid waste has negative health impacts, especially in developing countries, where more than 90% of waste is openly dumped or burned [9,10]. To achieve sustainability goals, it is desirable to use “clean manufacturing” procedures to gain “value-added” products from waste materials [11]. Kitchen biodegradable trash, such as vegetable and fruit peels and seeds, spent tea leaves, and juices, is abundant in the ecosystem that contaminates the environment. These wastes produce a lot of microbial flora in their vicinity, emit a foul odor, and act as sites for disease vectors such as mosquitos and rodents that spread diseases to humans [12]. One of the most important ways to get rid of this biodegradable waste, after recycling, is to use it as raw material in green synthesis. It is a renewable source that is sustainable, cheap, and easily available, with usual affluence [13]. Previously, numerous articles reported the synthesis of various NPs using waste products such as mango peel, orange, onion, pomegranate, sapota, rice husks, watermelon rind, coconut coir, eggshell, groundnut shell, tamarind shell, human hair, tea waste, marine waste, algal extract, and slaughterhouse waste [14].

Zinc oxide nanoparticles (ZnONPs) induce excess reactive oxygen species (ROS) within the cell: superoxide anion ($O_2^{\bullet-}$), hydrogen peroxide (H_2O_2), and hydroxyl radicals ($\bullet OH$). Therefore, it is known that ZnONPs act as an antibacterial agent due to their high activity to block a wide range of pathogens. ZnONPs were synthesized from extracts of *Punica granatum*, *Musa acuminata*, pineapple, dragon fruit (*Hylocereus polyrhizus*) peels, and longan (*Dimocarpus longan Lour*) seeds, which have a role in biology, biomedicine, environment, industries, agriculture, and food [14–17].

The use of the most abundant biomass, banana peels (BP) and date seeds (DS), in NPs' synthesis represents a low-cost, renewable, and eco-friendly route that could help in solving the pollution problem. In addition, biomass could be used in the large-scale production of various NPs. This route is a good alternative for NPs' synthesis, instead of physicochemical methods that are more expensive, need more instruments, and can generate toxic and hazardous effects in the environment.

The aim of the present study is to synthesize ZnONPs in an eco-friendly way by using biodegradable wastes (banana peels and date seeds). Characterization was completed using different techniques: ultraviolet–visible spectrophotometer (UV–VIS), scanning (SEM), transmission electron microscope (TEM), zeta potential analysis, X-ray diffraction (XRD), and Fourier-transform infrared (FTIR) spectroscopy to confirm ZnONPs' formation and determine their size, shape, and surface charge. In addition, green synthesized ZnONPs from two different waste extracts were used against four different bacterial strains, two Gram-positive (*Staphylococcus aureus* and *Bacillus subtilis*) and two Gram-negative (*Escherichia coli* and *Salmonella enteritidis*), to assess their antibacterial potential using the minimum inhibitory concentration (MIC) and minimum bactericidal concentration (MBC).

2. Materials and Methods

2.1. Banana Peel (BPE) and Date Seed (DSE) Extracts' Preparation

Fresh banana and dried date fruits were purchased from a local shop in Taif Governate, Saudi Arabia (KSA). Fruits were washed prior to their use. Then, banana peels were isolated, left covered until full dryness (for about 48 h, away from the sun), and finally ground using a domestic blender into fine powder. On the other hand, date seeds were collected and ground using a huge grinder (ALSAIF-ELEC, Model E03407, 220–240 V, 50/60 Hz, 1200 W, Guangdong, China). In two separate 250 mL flasks: 10 g of each powder, banana peel (BP) or date seed (DS), was added to 100 mL autoclaved distilled water, boiled for 10 min, filtered, and then cooled down at room temperature. Finally, we obtained banana peel (BPE) and date seed (DSE) extracts for further preparation. It was recorded that banana peel extract (BPE) is alkaline with a pH value of 9.91, but date seed (DSE) extract is approximately neutral with a pH value of 6.2.

2.2. Biosynthesis of Zinc Oxide Nanoparticles (ZnONPs)

Next, 95 mL of 0.01 M Zinc acetate dihydrate solution ($\text{Zn}(\text{C}_2\text{H}_3\text{O}_2)_2 \cdot 2\text{H}_2\text{O}$) (100% Grade, Mwt: 219.5 g/mol, Sigma-Aldrich, Saint-Louis, MO, USA) in sterile distilled water was separately mixed with 5 mL of each extract (BP or DS). Mixtures were heated at 70 °C for 1 h on a magnetic stirrer until the appearance of precipitates (Figure 1). For both prepared zinc oxide nanoparticles (ZnONPs_BPE and ZnONPs_DSE), part was kept in the aqueous form for further ultraviolet–visible (UV–vis) assessment, while the rest was dried at 60 °C overnight for other assessments [18,19].

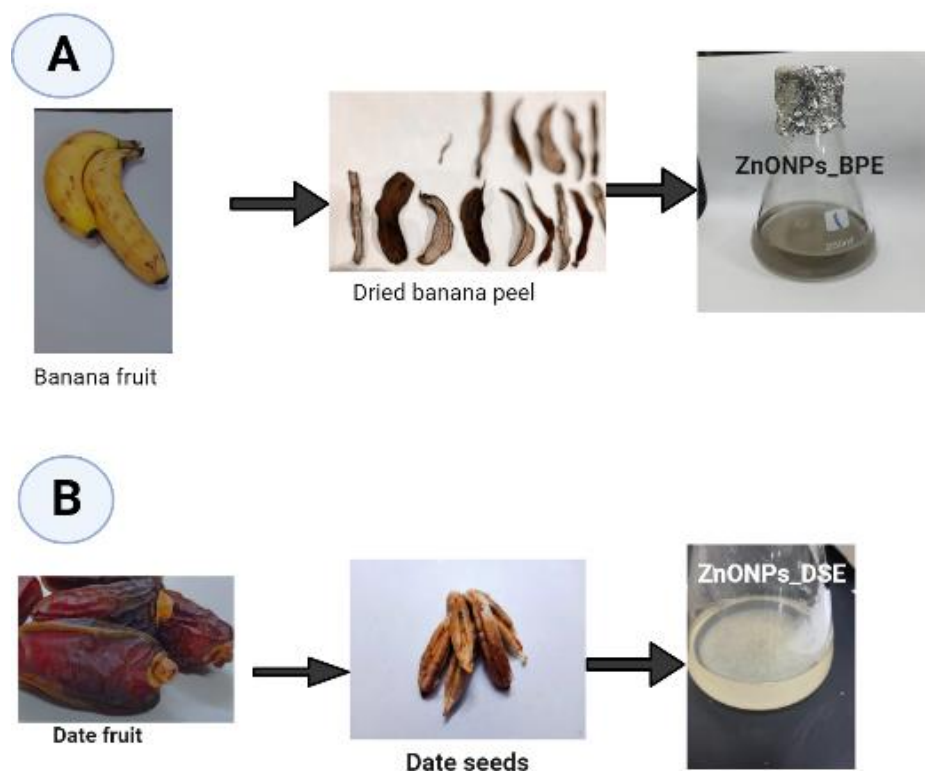


Figure 1. Schematic illustration of ZnONPs_BPE (A) and ZnONPs_DSE (B) preparation using banana peel extract and date seed extract, respectively. Created in BioRender.com with agreement number: RA25FWOA8Q, accessed on 30 May 2023.

2.3. Characterization of Prepared ZnONPs

2.3.1. UV–Vis Spectroscopy

Aqueous ZnONPs_BPE and ZnONPs_DSE nanoparticles were used for UV–vis measurement. The absorption spectra were determined at a wavelength range of 200–800 nm by using UV–VIS–NIR spectrophotometer (UV-1601, Shimadzu, Japan).

2.3.2. Surface Morphology, Charge, and Size Determination

Different techniques were used to determine the size, surface charge, and crystalline shape of biologically prepared ZnONPs_BPE and ZnONPs_DSE. For scanning electron microscope (SEM): ZnONPs powder (from both BPE and DSE extracts) was coated with carbon using Cressington Sputter Coater (108auto, thickness controller MTM-10, Watford, UK) for 10 min prior to scanning (20 kV, JEOL JSM-6390LA, Analytical Scanning Electron Microscope, at Electron Microscope Unit of Taif University) with different magnifications. A transmission electron microscope (TEM, JEOL–JSM-1400 PLUS, Tokyo, Japan, at 100 kV) was used for size and crystalline structure determination. Photos obtained by TEM were analyzed by ImageJ software to determine the synthesized nanoparticles' average size. X-ray diffractometer (XRD) spectra were recorded by $\text{CuK}\alpha$ radiation (at 30 kV and 100 mA) with a wavelength of 1.5406 Å in the 2θ (20°–80°). Patterns of XRD

were plotted by OriginLab software[®] (2018). The surface charge of ZnONPs was evaluated by using Dynamic Light Scattering (DLS) (Zetasizer Nano ZS, Malvern Instruments Ltd., Malvern, UK) at a fixed angle of 173° at 25 °C. Finally, 1 mg of each sample was dispersed in 1 mL deionized water and then sonicated for 10 min before measurement.

2.3.3. Fourier-Transform Infrared (FTIR) Spectroscopy

Fourier-transform infrared (FTIR, Agilent Technologies) spectroscopy was used at wavelength of 450–4000 cm⁻¹ to determine the possible functional groups that are responsible for the synthesis, capping, and stabilization of ZnONPs.

2.4. Antimicrobial Assessment

The antimicrobial potential of the green synthesized ZnO nanoparticles was determined by the standard methods of the Clinical and Laboratory Standards Institute (CLSI). All bacterial strains were obtained from Nawah Scientific Inc. (Mokatam, Cairo, Egypt).

2.4.1. Preparing Inoculum (Colony Suspension Method)

A disc of each *Escherichia coli* ATCC 8739, *Staphylococcus aureus* ATCC 6538, *Salmonella enteritidis* ATCC 13076, and *Bacillus subtilis* ATCC 6633 was inoculated into 100 mL of tryptic soy broth medium and incubated at 35.0 °C ± 1.0 for 24.0 h. For the preparation of a fresh culture agar plate (18–24 h), a loopful from the broth was streaked onto an appropriate non-selective medium (tryptic soy agar) and then incubated at the same previous temperature. A direct sterile saline solution was prepared by inoculating 3–4 colonies (from the organism plate), and the suspension was adjusted to achieve a turbidity equivalent to a 0.5 McFarland standard of each strain using DensiCHEK[®] optical device. This adjustment results in a suspension containing approximately 1–2 × 10⁸ CFU/mL. The suspension was diluted by inoculating 1.0 mL of inoculum into 20 mL of Muller Hinton broth, which resulted in a concentration of approximately 1.0 × 10⁶ colony-forming unit/milliliter CFU/mL [20].

2.4.2. Broth Microdilution Method

Serial two-fold dilutions of zinc oxide nanoparticles (ZnONPs_BPE and ZnONPs_DSE, each separately) in concentrations ranging from 3 mg/mL to 0.005 mg/mL were used. First, 200 µL from the ZnONPs' sample was directly inoculated in the first well of the 96-well plate (without dilution). Then, 100 µL of Muller Hinton Broth (MHB) was consequently inoculated in the remaining wells. Next, 100 µL from the first well was aspirated, transferred to the next well (previously filled with 100 µL MHB) to make a 1:2 dilution, and mixed well, and then 100 µL was aspirated from 1:2 dilution using a new tip and added to the next 100 µL broth (1:4 dilution); this step was repeated for preparing 9 dilutions for each sample. Later, 10 µL of previously prepared inoculum was added to each well, which should result in a final concentration of 5.0 × 10⁵ (CFU/mL) (the recommended concentration is 2–8 × 10⁵ CFU/mL). Another 10 µL from each organism suspension was diluted and cultured (externally) to confirm inoculum density. A growth control well containing inoculated broth, without a sample, was added to each sample/plate. A negative control well containing only the broth without a sample or bacteria was added to each sample plate. Finally, all the plates were incubated at 35.0 ± 1.0 °C for 24.0 ± 2.0 h [20].

2.4.3. Quality Control Results

After incubation, plates were removed from the incubator and placed on a dark surface to check growth. All growth control wells yielded turbid solution of growth, indicating the validity of the test. All blank wells were clear, indicating the validity of the test. Inoculum density culture results were confirmed to have a 4–6 × 10⁵ CFU/mL concentration for the tested organism [20].

2.4.4. MIC and MBC Determination

The minimum inhibitory concentration (MIC) and minimum bactericidal concentration (MBC) of ZnONPs_BPE and ZnONPs_DSE against four different strains (*Escherichia coli*, *Staphylococcus aureus*, *Salmonella enteritidis*, and *Bacillus subtilis*) were completed. The MIC endpoint was the lowest concentration of ZnONPs where no visible growth was seen in the tubes. After the MIC determination, MBC was completed as a complementary step. Aliquots of 50 μ L from all the serial dilutions that showed no visible bacterial growth were seeded on agar plates and incubated (37 °C, 24 h). MBC endpoint indicated the lowest concentration of ZnO nanoparticles that killed at least 99.9% of the bacterial population.

2.4.5. Statistical Analysis

The MBC result of ZnONPs_BPE and ZnONPs_DSE on four different strains was analyzed by one-way ANOVA test. The significance of all the statistical tests was determined at $p < 0.05$ using GraphPad Prism 8.0.1 software (GraphPad® 2017, San Diego, CA, USA).

3. Results and Discussion

3.1. Characterization of ZnONPs

3.1.1. Color Change and UV–Vis Spectroscopy of ZnONPs

Two different aqueous extracts, BPE and DSE, were used for the synthesis of ZnONPs. After the addition of zinc acetate dihydrate and incubation at 70 °C, the clear BPE and DSE extracts turned to dark gray and dark yellow, respectively, which indicates Zn²⁺ reduction to form ZnONPs (Figure 1). The change in color represents the initial confirmation of NPs' formation. This was confirmed by UV–Vis spectroscopy at a 200–800 nm range. Figure 2 shows a UV–visible spectral analysis of the green synthesized ZnONPs_BPE, with a strong absorption peak at 290 nm, and of ZnONPs_DSE with a broad band at 400 nm. Likewise, previous studies of green ZnONPs' synthesis reported the same range (258 nm–399 nm) using different plant extracts such as sea lavender (*Limonium pruinatum* L. Chaz.), *Punica granatum* L. peel, coffee ground, *Elaeagnus angustifolia* L. leaf, and *Coriandrum sativum* extracts [19,21–23].

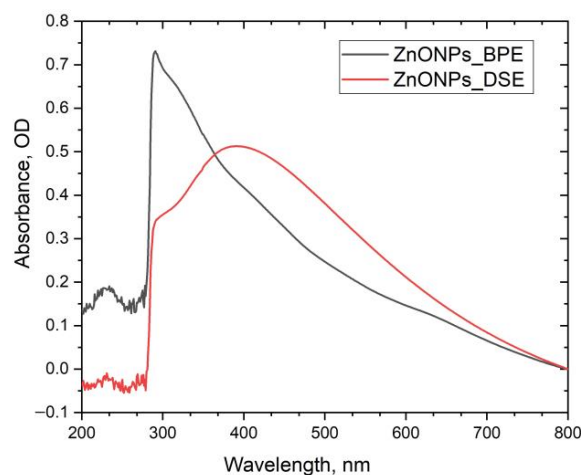


Figure 2. UV–visible spectral analysis of green synthesized ZnONPs using banana peel and date seed extracts.

In the present study, we selected banana peel, the fourth-most-significant foodstuff globally, and date seed, the most important biodegradable waste in Saudi Arabia, in the synthesis of ZnONPs. These agro-wastes comprise important components such as cellulose, hemicellulose, lignin, flavonoids, phenolics, and other phytochemical components. Such components are responsible for the reduction, synthesis, capping, and stabilization of ZnONPs [24,25]. There was a significant shift of spectra between ZnONPs_BPE (290 nm) and ZnONPs_DSE (400 nm) due to a change in their surface plasmon resonance

that is affected by nanoparticle size or the capping of the phytochemicals present in the extract [19,23]. There was a shift of the absorption edge to a lower wavelength (UV), as the nanoparticle size decreased [23].

3.1.2. Shape, Size, and Surface Charge of Zinc Oxide Nanoparticles

The morphology, shape, size, and surface charge of the green synthesized ZnONPs were investigated using SEM, TEM, XRD, and zeta potential. Figure 3 shows the nanostructure of green synthesized ZnONPs_BPE with mean size = 57.4 ± 13.8 nm using the TEM image analyzed by ImageJ. On the other hand, the SEM image revealed the agglomeration of ZnONPs_BPE due to the low negativity charge present on its surfaces, with average zeta potential distribution = -9.62 mV.

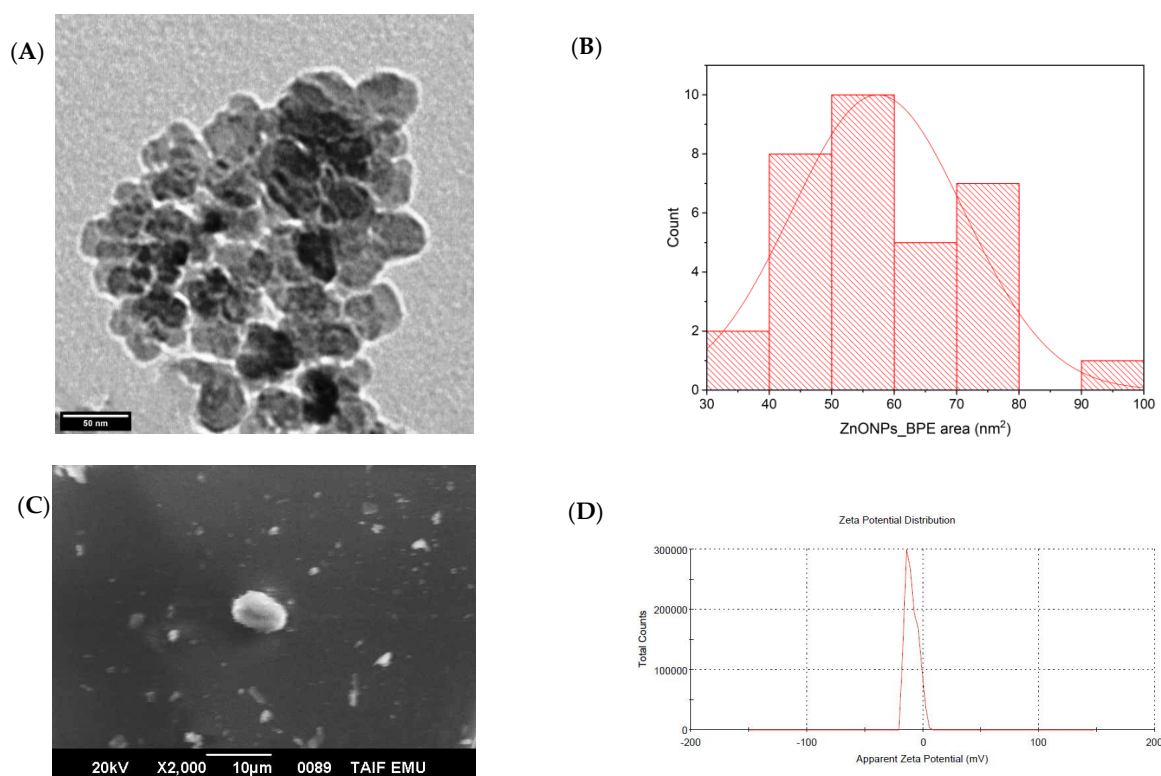


Figure 3. Transmission electron microscope photo of ZnONPs_BPE, 50 nm scale bar (A). Histogram showing NPs' mean size by ImageJ software (mean size = 57.4 ± 13.8 nm) (B). SEM image (C) shows separate nanocrystalline and other interlinked shapes of ZnONPs at 2000 \times , 10 μ m scale bar. Surface charge of ZnONPs_BPE = -9.62 mV (D).

The TEM image of ZnONPs_DSE shows its nanoscale size with mean size = 72.6 ± 17.1 nm. On the contrary, the SEM image reported the accumulation of ZnONPs_DSE to form small and large chunky particles due to the lower surface negativity of NPs with average zeta potential distribution = -5.69 mV (Figure 4).

It is clear that ZnONPs_BPE (57.4 ± 13.8 nm) has a smaller size than ZnONPs_DSE (72.6 ± 17.1), as previously reported by their UV spectral shift. The change in their sizes might be attributed to the differences in negativity charges present on their surfaces [18], in which lower negativity (-5.69 mV of ZnONPs_DSE) leads to more aggregation of nanoparticles to produce a larger one.

The XRD profiles of both ZnONPs_BPE and ZnONPs_DSE showed the same sharp and distinct peaks of 2 Theta at 31.7° (plane 100), 34.4° (002), 36.2° (101), 47.5° (102), 56.6° (110), 62.8° (103), 66.38° (200), 67.9° (112), and 69° (201) (Figure 5). The XRD pattern revealed that ZnONPs have a hexagonal crystalline shape according to the Joint Committee on Power Diffraction (JCPD) standards, card number (36-1451). Therefore, the XRD data

are consistent with the TEM images of ZnONPs_BPE and ZnONPs_DSE, confirming their hexagonal crystalline shape.

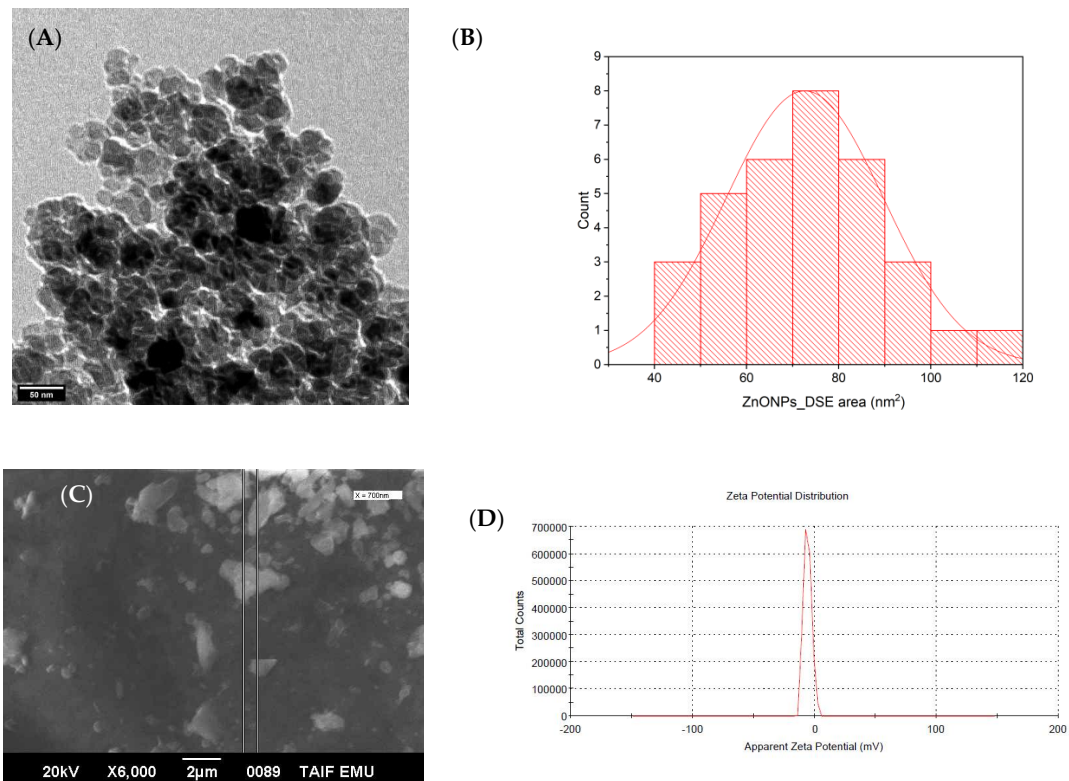


Figure 4. Transmission electron microscope photo of ZnONPs_DSE, 50 nm scale bar (A). Histogram showing NPs' mean size by ImageJ software (mean size = 72.6 ± 17.1 nm) (B). SEM image (C) shows small and large non-homogenous nanoparticles of ZnONPs at 6000 \times , 2 μ m scale bar. Mean zeta potential distribution of ZnONPs_DSE = -5.69 mV (D).

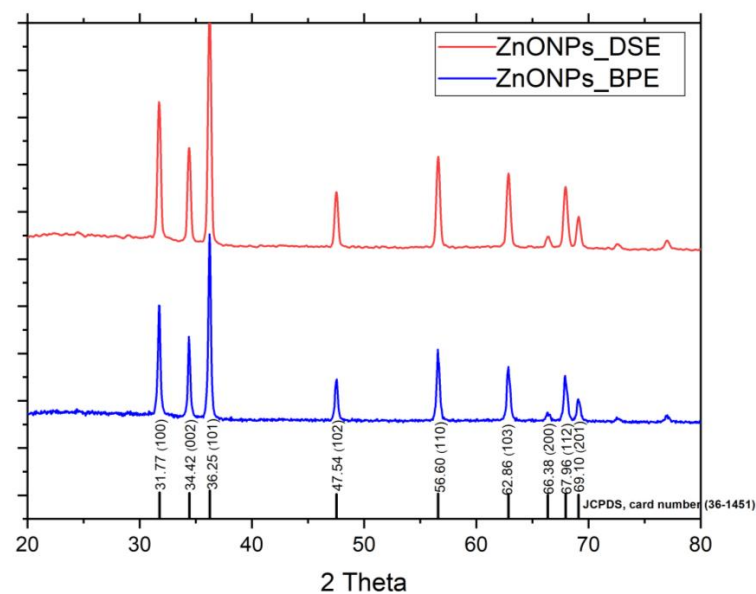


Figure 5. XRD patterns of green synthesized ZnONPs by using BP and DS extracts in comparison to JCPDS, card number (36-1451). Both patterns show sharp peaks at the same 2 Theta.

The present results are consistent with a previous work: Aminuzzaman et al. [26] synthesized ZnONPs using an aqueous extract of dragon fruit (*Hylocereus polyrhizus*) peel

biowaste as a reducing and stabilizing agent. Their TEM and XRD analyses showed ZnONPs with an average size of 56 nm that were well-crystalline and possessed a wurtzite hexagonal phase. Moreover, Chankaew et al. [17] synthesized green ZnONPs using longan seeds (*Dimocarpus longan* Lour) with NPs' sizes ranging between 40–60 and 40–80 nm. The XRD pattern confirmed their hexagonal phase, but their shape was mostly irregular according to the TEM results, while another study showed smaller-sized green synthesized ZnONPs = 26 nm using *Elaeagnus angustifolia* L. leaf extracts [22]. The variation in the ZnONPs' size was attributed to changes in the used zinc acetate (precursor) concentration and/or reaction temperature [17].

3.1.3. FTIR Analysis

FTIR spectroscopy helps to identify the main functional groups found in BP and DS extracts that participate in the synthesis, capping, and stabilization of ZnONPs. Figure 6 shows the FTIR absorption spectra of ZnONPs_BPE and ZnONPs_DSE within the range of 4000–450 cm^{-1} . We determined similar/near peaks and bands between ZnONPs_BPE and ZnONPs_DSE, which indicates that both extracts (banana peel and date seed) have similar functional groups of their phytochemicals. The peaks at 3313.4 and 3367 cm^{-1} are attributed to O–H stretching vibrations in the hydroxyl groups. C–H stretching of the alkane, methyl and methylene groups appears at 2920.3 cm^{-1} (for ZnONPs_BPE) and at 2924 cm^{-1} (ZnONPs_DSE). These absorption bands show contributions from the cellulose, hemicellulose, and lignin found in extracts. The observed peaks at 1734 cm^{-1} and 1744 cm^{-1} are assigned to the C=O stretching vibrations of the carboxylic groups (-COOH, -COOCH₃) of the ferulic and p-coumaric acids of lignin and/or hemicelluloses. The peaks at 1616 cm^{-1} and 1613.6 cm^{-1} may represent C=C or C=N vibrations in the aromatic region. The peaks observed at 1377 cm^{-1} and 1364 cm^{-1} –1248 cm^{-1} can be attributed to the C-H bending of crystalline cellulose hemicelluloses or lignin polymer [27–29].

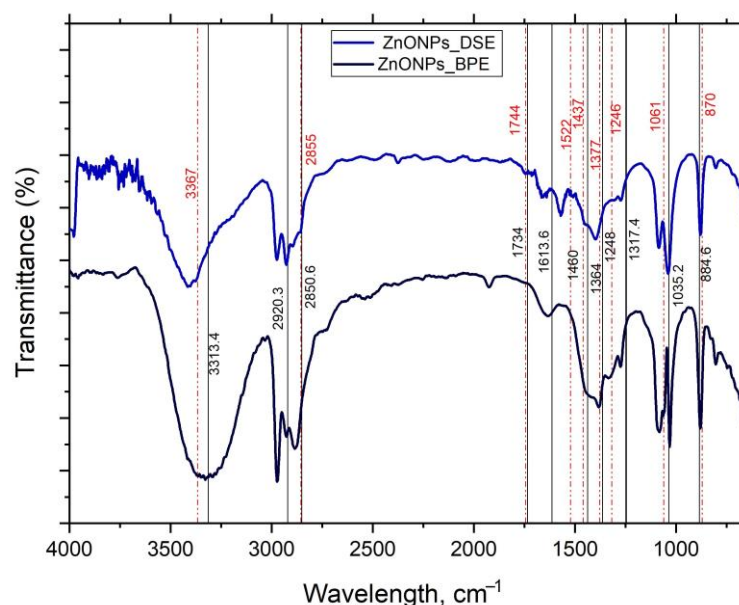


Figure 6. FTIR spectra of green synthesized ZnONPs_BPE and ZnONPs_DSE.

3.2. Antimicrobial Potential of ZnONPs

Recently, antibiotic resistance has grown at an alarming rate in all parts of the world. Therefore, biogenic ZnONPs have been developed for antibacterial use. ZnONPs_BPE and ZnONPs_DSE have antibacterial potential against various bacterial strains: Gram-negative (*Escherichia coli* ATCC 8739 and *Salmonella enteritidis* ATCC 13076) and Gram-positive (*Bacillus subtilis* ATCC 6633 and *Staphylococcus aureus* ATCC 6538) (Supplementary File). Table 1 shows that ZnONPs-BPE has a higher antimicrobial effect against *Salmonella*

enteritidis (MIC = 0.75 mg/mL, MBC = 1.5 mg/mL), while ZnONP_DSE has a higher antimicrobial effect against *Staphylococcus aureus* (MIC = 0.75 mg/mL, MBC = 3 mg/mL). The present results agree with previous studies, in which Iqbal et al. [22] reported the antimicrobial potential of ZnONPs from *Elaeagnus angustifolia* L. leaf extracts against *E. coli* ATCC 15224, *S. aureus* ATCC 25923, *P. aeruginosa* ATCC 9721, *K. pneumoniae* ATCC 4617, and *B. subtilis* ATCC 6633 at concentrations ranging from 37.5 to 1200 $\mu\text{g mL}^{-1}$.

Table 1. Minimum inhibitory concentration (MIC) and minimum bactericidal concentrations (MBC) of ZnONPs_BPE and ZnONPs_DSE (unit in mg/mL).

Bacterial Strain	ZnONPs_BPE		ZnONPs_DSE	
	MIC	MBC	MIC	MBC
<i>Escherichia coli</i> ATCC 8739	1.5	>3	1.5	1.5
<i>Staphylococcus aureus</i> ATCC 6538	1.5	>3	0.75	3
<i>Bacillus subtilis</i> ATCC 6633	1.5	>3	1.5	3
<i>Salmonella enteritidis</i> ATCC 13076	0.75	1.5	1.5	1.5

Previous studies reported that the bactericidal activity of ZnONPs could be due to their ability to perforate the microbial cell membrane to produce ROS that damage microbial DNA [30]. Furthermore, due to their nanoscale size, ZnONPs can efficiently enter microbial cell membranes through small pores and may cause an imbalance of minerals, which in turn leads to the leakage of intracellular proteins and enzymes, inhibits cell growth, and finally leads to cell death [31]. Zinc nanoparticles have strong bactericidal capabilities against both Gram-positive and Gram-negative bacteria [32,33]. ZnONPs release zinc ions that impair the cell membrane function by causing ion concentration differences, which block material transport in which positively charged zinc oxide (ZnO) directly binds to the negatively charged bacterial cell walls that in turn denature proteins by reacting with functional groups. In addition, ZnO induces a large number of free radicals (OH^- , H_2O_2 , and O^{2-}) under UV or visible light. These free radicals destroy the bacterial cell wall, enter the cell, damage DNA, and finally lead to bacterial death [30] (Figure 7).

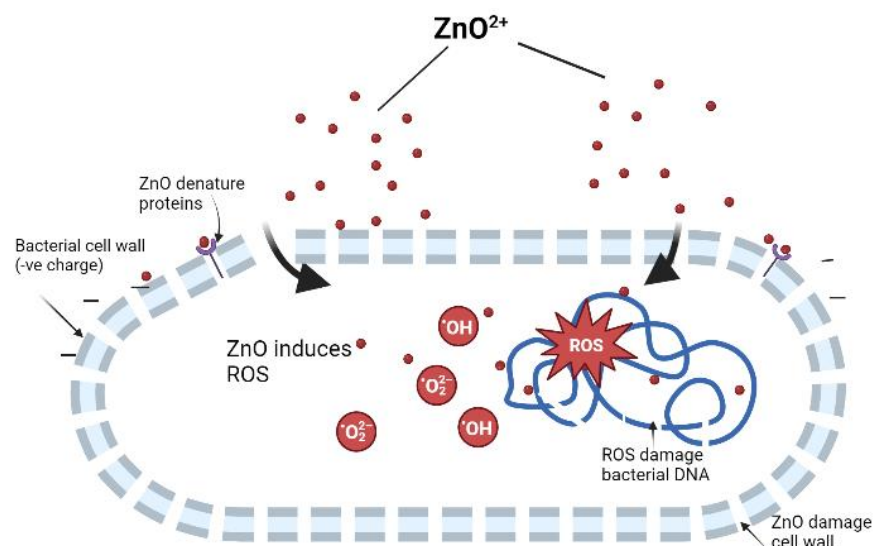


Figure 7. Schematic illustration of the suggested mechanism of the bactericidal potential of green synthesized ZnONPs. Created in BioRender.com with agreement number: WW25FWO1Q5, accessed on 30 May 2023.

Moreover, the bactericidal potential of green synthesized ZnONPs may be due to the bioactive molecules, from BP and DS extracts, adsorbed onto the NP surface. BP has high levels of pectin and phytochemicals (0.90–3.0 g/100 g dry weight) such as ascorbic acid, β -carotene, tocopherol, and gallic acid [34,35]. We studied examples of both Gram-positive (*Bacillus subtilis* and *Staphylococcus aureus*) and Gram-negative (*Escherichia coli* and

Salmonella enteritidis) strains. Gram-positive bacteria have a peptidoglycan layer, whereas Gram-negative bacteria have an additional lipopolysaccharide layer, which makes their cell wall highly impermeable to lipophilic solutes compared to Gram-positive bacteria [36]. ZnONPs-BPE has a higher antimicrobial effect against Gram-negative *Salmonella enteritidis* than other strains. It was reported that the aqueous extract of BP is more effective than all other extracts of banana plants (leaves, flowers, pseudo-stem, corm, and root) against various bacterial strains [37]. An aqueous extract of BP inhibited the growth of Gram-negative bacteria (*P. aeruginosa*) [38]. On the other hand, all banana plant extracts using ethyl acetate and methanol show different degrees of inhibition, the MIC is dose- and solvent-dependent, and it was reported that Gram-negative bacteria are the most vulnerable to inhibition [39]. ZnONP_DSE has a higher effect against Gram-positive bacteria (*Staphylococcus aureus*). It was reported that DS contains polyphenols, flavonoids, alkaloids, tannins, and steroids that significantly retard microbial growth, proliferation, and infection [40]. Their antibacterial efficiency differs according to the type of date, organic solvent, target organism, and plant parts used [41]. However, a methanolic extract of Ajwa date seeds had antibacterial activity against *E. coli*, *Bacillus cereus*, *S. aureus*, and *Serratia marcescens* [42].

Therefore, using renewable biomass as the raw material for NPs' synthesis was considered a low-cost and sustainable option that could help solve local and global pollution [43]. For example, rice husks (or rice hulls) contain high amounts of cellulose, hemicellulose, and lignin used to synthesize SiO₂ [44], nanoporous MnO₂ [45], and Mg₂SiO₄ [46] nanomaterials that have various applications such as in the biomedical fields [43], as an electrode material for high-performance supercapacitors, and as a green additive for sustainable concrete production [47]. In addition, sugar cane bagasse, bamboo leaf, eggshell, walnut shell, wheat straw, coconut shell, banana peel, tea waste, and other miscellaneous agricultural wastes that are abundantly available could be used in various NPs' syntheses [43]. Finally, biomass-derived nanoparticle synthesis opened a novel window to innovate new routes in the clean, eco-friendly, and large-scale synthesis of thoroughly purified, morphologically well-defined nanoparticles [43].

4. Conclusions

In the present study, ZnONPs were successfully prepared using two different extracts (banana peel and date seed) as potential reducing, capping, and stabilizing agents. The XRD results indicate that the formed ZnONPs possessed a hexagonal wurtzite phase. ZnONPs_BPE (57.4 ± 13.8 nm) appears smaller in size in comparison to ZnONPs_DSE (72.6 ± 17.1 nm), by using TEM. ZnONPs appeared with agglomeration due to the low negativity that is found on their surfaces from used extracts. FTIR confirms the presence of the main functional groups in the phytochemicals found in the extracts that help in ZnONPs' synthesis and stabilization. Finally, the biosynthesized ZnONPs demonstrated a good antimicrobial potential against both the selected Gram-positive and Gram-negative strains. Further studies are needed to assess their biocompatibility, in vitro and in vivo, and mechanistic studies are needed to evaluate their safety and nano-pharmacological relevance in multiple bioactivities.

Supplementary Materials: The following supporting information can be downloaded at: <https://www.mdpi.com/article/10.3390/su15119048/s1>, Figure S1: Effect of ZnONPs_BPE on *Escherichia coli* ATCC 8739, *Staphylococcus aureus* ATCC 6538, *Bacillus subtilis* ATCC 6633, and *Salmonella enteritidis* ATCC 13076. Figure S2: Effect of ZnONPs_DSE on *Escherichia coli* ATCC 8739, *Staphylococcus aureus* ATCC 6538, *Bacillus subtilis* ATCC 6633, and *Salmonella enteritidis* ATCC 13076. Table S1: MIC reading Figure S1 shows effect of ZnONPs_BPE on *Escherichia coli* ATCC 8739, *Staphylococcus aureus* ATCC 6538, *Bacillus subtilis* ATCC 6633, and *Salmonella enteritidis* ATCC 13076. Table S2: MIC reading Figure S1 shows effect of ZnONPs_DSE on *Escherichia coli* ATCC 8739, *Staphylococcus aureus* ATCC 6538, *Bacillus subtilis* ATCC 6633, and *Salmonella enteritidis* ATCC 13076.

Funding: The researchers would like to acknowledge Deanship of Scientific Research, Taif University, for funding this work.

Institutional Review Board Statement: Not applicable.

Informed Consent Statement: Not applicable.

Data Availability Statement: All data generated or analyzed during this study are included in this published article.

Acknowledgments: The researchers would like to acknowledge Deanship of Scientific Research, Taif University, for funding this work.

Conflicts of Interest: The authors declare no conflict of interest.

References

1. Dos Santos, C.A.; Seckler, M.M.; Ingle, A.P.; Gupta, I.; Galdiero, S.; Galdiero, M.; Gade, A.; Rai, M. Silver nanoparticles: Therapeutic uses, toxicity, and safety issues. *J. Pharmacol. Sci.* **2014**, *103*, 1931–1944. [CrossRef]
2. Chowdhury, M.A.; Hossain, N.; Kchaou, M.; Nandee, R.; Shuvho, M.B.A.; Sultana, S. Scope of eco-friendly nanoparticles for anti-microbial activity. *Curr. Opin. Green Sustain. Chem.* **2021**, *4*, 100198. [CrossRef]
3. Pal, K.; Chakroborty, S.; Nath, N. Limitations of nanomaterials insights in green chemistry sustainable route: Review on novel applications. *Green Process. Synth.* **2022**, *11*, 951–964. [CrossRef]
4. Fariq, A.; Khan, T.; Yasmin, A. Microbial synthesis of nanoparticles and their potential applications in biomedicine. *J. Appl. Biomed.* **2017**, *15*, 241–248. [CrossRef]
5. Harshiny, M.; Matheswaran, M.; Arthanareeswaran, G.; Kumaran, S.; Rajasree, S. Enhancement of antibacterial properties of silver nanoparticles-ceftriaxone conjugate through Mukiamaderaspatana leaf extract mediated synthesis. *Ecotoxicol. Env. Saf.* **2015**, *121*, 135–141. [CrossRef] [PubMed]
6. Begum, S.J.P.; Pratibha, S.; Rawat, J.M.; Venugopal, D.; Sahu, P.; Gowda, A.; Qureshi, K.A.; Jaremko, M. Recent advances in green synthesis, characterization, and applications of bioactive metallic nanoparticles. *Pharmaceuticals* **2022**, *15*, 455. [CrossRef]
7. Doble, M.; Kruthiventim, A.K. *Green Chemistry and Engineering*; Academic Press: Cambridge, MA, USA, 2007.
8. Aguilar, Z. *Nanomaterials for Medical Applications*; Elsevier: Boston, MA, USA, 2013.
9. UNEP. Solid Waste Management | UNEP—UN Environment Programme. Available online: <https://www.unenvironment.org/explore-topics/resource-efficiency/what-we-do/cities/solid-waste-management> (accessed on 10 May 2020).
10. Abdelbasir, S.M.; McCourt, K.M.; Lee, C.M.; Vanegas, D.C. Waste-Derived Nanoparticles: Synthesis Approaches, Environmental Applications, and Sustainability Considerations. *Front. Chem.* **2020**, *8*, 782. [CrossRef] [PubMed]
11. Ferronato, N.; Torretta, V. Waste mismanagement in developing countries: A review of global issues. *Int. J. Environ. Res. Public Health* **2019**, *16*, 1060. [CrossRef]
12. Huston, M.; DeBella, M.; DiBella, M.; Gupta, A. Green synthesis of nanomaterials. *Nanomaterials* **2021**, *11*, 2130. [CrossRef]
13. Siwal, S.S.; Zhang, Q.; Devi, N.; Saini, A.K.; Saini, V.; Pareek, B.; Gaidukovs, S.; Thakur, V.K. Recovery processes of sustainable energy using different biomass and wastes. *Renew Sustain. Energy Rev.* **2021**, *150*, 111483. [CrossRef]
14. Aswathi, V.P.; Meera, S.; Maria, C.G.A.; Nidhin, M. Green synthesis of nanoparticles from biodegradable waste extracts and their applications: A critical review. *Nanotechnol. Environ. Eng.* **2022**. [CrossRef]
15. Saffar, R.; Athira, P.V.; Kalita, K.; Manuel, S.G.; Pradeep, N. Nanoparticle synthesis from biowaste and its potential as an antimicrobial agent. *Res. Artic.* **2021**. [CrossRef]
16. Hassan-Basri, H.; Talib, R.A.; Sukor, R.; Othman, S.H.; Ariffin, H. Effect of synthesis temperature on the size of ZnO nanoparticles derived from pineapple peel extract and antibacterial activity of ZnO–starch nanocomposite films. *Nanomaterials* **2020**, *10*, 1061. [CrossRef] [PubMed]
17. Chankaew, C.; Tapala, W.; Grudpan, K.; Rujiwatra, A. Microwave synthesis of ZnO nanoparticles using longan seeds biowaste and their efficiencies in photocatalytic decolorization of organic dyes. *Environ. Sci. Pollut. Res.* **2019**, *26*, 17548–17554. [CrossRef]
18. Abdelmigid, H.M.; Morsi, M.M.; Hussien, N.A.; Alyamani, A.A.; Al Sufyani, N.M. Comparative Analysis of nanosilver Particles synthesized by different approaches and their antimicrobial efficacy. *J. Nanomater.* **2021**, *2021*, 2204776. [CrossRef]
19. Abdelmigid, H.M.; Hussien, N.A.; Alyamani, A.A.; Morsi, M.M.; AlSufyani, N.M.; Kadi, H.A. Green Synthesis of Zinc Oxide Nanoparticles Using Pomegranate Fruit Peel and Solid Coffee Grounds vs. Chemical Method of Synthesis, with Their Biocompatibility and Antibacterial Properties Investigation. *Molecules* **2022**, *27*, 1236. [CrossRef]
20. European Committee for Antimicrobial Susceptibility Testing (EUCAST) of the European Society of Clinical Microbiology and Infectious Diseases (ESCMID). Determination of minimum inhibitory concentrations (MICs) of antibacterial agents by broth dilution. *Clin. Microbiol. Infect.* **2003**, *9*, ix–xv. [CrossRef]
21. Naiel, B.; Fawzy, M.; Halmy, M.W.A.; Mahmoud, A.E.D. Green synthesis of zinc oxide nanoparticles using Sea Lavender (*Limonium prinosum* L. Chaz.) extract: Characterization, evaluation of anti-skin cancer, antimicrobial and antioxidant potentials. *Sci. Rep.* **2022**, *12*, 20370. [CrossRef]
22. Iqbal, J.; Abbasi, B.A.; Yaseen, T.; Zahra, S.A.; Shahbaz, A.; Shah, S.A.; Uddin, S.; Ma, X.; Raouf, B.; Kanwal, S.; et al. Green synthesis of zinc oxide nanoparticles using *Elaeagnus angustifolia* L. leaf extracts and their multiple in vitro biological applications. *Sci. Rep.* **2021**, *11*, 20988. [CrossRef]

23. Singh, J.; Kaur, S.; Kaur, G.; Basu, S.; Rawat, M. Biogenic ZnO nanoparticles: A study of blueshift of optical band gap and photocatalytic degradation of reactive yellow 186 dye under direct sunlight. *Green Process. Synth.* **2019**, *8*, 272–280. [[CrossRef](#)]
24. Marfu'ah, S.; Rohma, S.M.; Fanani, F.; Hidayati, E.N.; Nitasari, D.W.; Primadi, T.R.; Ciptawati, E.; Sumari, S.; Fajaroh, F. Green Synthesis of ZnO Nanoparticles by Using Banana Peel Extract as Capping agent and Its Bacterial Activity. *IOP Conf. Ser. Mater. Sci. Eng.* **2020**, *833*, 012076. [[CrossRef](#)]
25. Rambabu, K.; Bharath, G.; Banat, F.; Show, P.L. Biosorption performance of date palm empty fruit bunch wastes for toxic hexavalent chromium removal. *Environ. Res.* **2020**, *187*, 109694. [[CrossRef](#)] [[PubMed](#)]
26. Aminuzzaman, M.; Ng, P.S.; Goh, W.-S.; Ogawa, S.; Watanabe, A. Value-adding to dragon fruit (*Hylocereus polyrhizus*) peel biowaste: Green synthesis of ZnO nanoparticles and their characterization. *Inorg. Nano-Met. Chem.* **2019**, *49*, 401–411. [[CrossRef](#)]
27. Socrates, G. *Infrared Characteristic Group Frequencies*; Wiley–Interscience Publication: New York, NY, USA, 1980.
28. Gnanasambandam, P.A.R. Determination of pectin degree of esterification by diffuse reflectance Fourier transform infrared spectroscopy. *Food Chem.* **2000**, *68*, 327–332. [[CrossRef](#)]
29. Li, X.F.T.; Yang, H.; Zhao, Y. Novel modified pectin for heavy metal adsorption. *China Chem. Lett.* **2007**, *18*, 325–328. [[CrossRef](#)]
30. Li, Y.; Xia, X.; Hou, W.; Lv, H.; Liu, J.; Li, X. How Effective are Metal Nanotherapeutic Platforms Against Bacterial Infections? A Comprehensive Review of Literature. *Int. J. Nanomed.* **2023**, *18*, 1109–1128. [[CrossRef](#)]
31. Mahdavi, B.; Saneei, S.; Qorbani, M.; Zhaleh, M.; Zangeneh, A.; Zangeneh, M.M.; Pirabbasi, E.; Abbasi, N.; Ghaneialvar, H. Ziziphora clinopodioides Lam. leaves aqueous extract mediated synthesis of zinc nanoparticles and their antibacterial, antifungal, cytotoxicity, antioxidant, and cutaneous wound healing properties under in vitro and in vivo conditions. *Appl. Organomet. Chem.* **2019**, *33*, e5164. [[CrossRef](#)]
32. Devanand Venkatasubbu, G.; Ramakrishnan, V.; Kumar, J. Nanocrystalline hydroxyapatite and zinc-doped hydroxyapatite as carrier material for controlled delivery of ciprofloxacin. *3 Biotech* **2011**, *1*, 173–186. [[CrossRef](#)]
33. Wang, Y.W.; Cao, A.; Jiang, Y.; Zhang, X.; Liu, J.-H.; Liu, Y.; Wang, H. Superior antibacterial activity of zinc oxide/graphene oxide composites originating from high zinc concentration localized around bacteria. *ACS Appl. Mater. Interfaces* **2014**, *6*, 2791–2798. [[CrossRef](#)]
34. Padam, B.S.; Tin, H.S.; Chye, F.Y.; Abdullah, M.I. Banana by-products: An under utilized renewable food biomass with great potential. *J. Food Technol. Res.* **2014**, *51*, 3527–3545. [[CrossRef](#)]
35. Khawas, P.; Deka, S.C. Encapsulation of natural antioxidant compounds from culinary banana by Cocrystallization. *J. Food Process. Preserv.* **2017**, *41*, e13033. [[CrossRef](#)]
36. Colco, R. Gram staining. In *Current Protocols in Microbiology*; John Wiley & Sons: Hoboken, NJ, USA, 2005. [[CrossRef](#)]
37. Norfaradhiah, R.; Rapeah, S. Antibacterial activity of water and methanol extracts of banana pulps against *Vibrio cholera*. *J. Environ. Health* **2017**, *8*, 86–103.
38. Evbuomwan, L.; Onodje, G.O.; Jacob, I.; Patric, C.E. Evaluating the antibacterial activity of *Musa acuminata* (banana) fruit peels against multidrug resistant bacterial isolates. *Int. J. Nov. Res. Life Sci.* **2018**, *5*, 26–31.
39. Mostafa, H.S. Banana plant as a source of valuable antimicrobial compounds and its current applications in the food sector. *J. Food Sci.* **2021**, *86*, 3778–3797. [[CrossRef](#)] [[PubMed](#)]
40. Amira, E.; Behija, S.E.; Bellig, M.; Lamia, L.; Manel, I.; Mohamed, H.; Lotfi, A. Effects of the ripening stage on phenolic profile, phytochemical composition and antioxidant activity of date palm fruit. *J. Agric. Food Chem.* **2012**, *60*, 10896–10902. [[CrossRef](#)]
41. Hussain, M.I.; Semreen, M.H.; Shanableh, A.; Khattak, M.N.K.; Saadoun, I.; Ahmady, I.M.; Mousa, M.; Darwish, N.; Radeef, W.; Soliman, S.S.M. Phenolic Composition and Antimicrobial Activity of Different Emirati Date (*Phoenix dactylifera* L.) Pits: A Comparative Study. *Plants* **2019**, *8*, 497. [[CrossRef](#)] [[PubMed](#)]
42. Samad, M.A.; Hashim, S.H.; Simarani, K.; Yaacob, J.S. Antibacterial properties and effects of fruit chilling and extract storage on antioxidant activity, total phenolic and anthocyanin content of four date palm (*Phoenix dactylifera*) cultivars. *Molecules* **2016**, *21*, 419. [[CrossRef](#)] [[PubMed](#)]
43. Zamani, A.; Marjani, A.; Mousavi, Z. Agricultural waste biomass-assisted nanostructures: Synthesis and application. *Green Process. Synth.* **2019**, *8*, 421–429. [[CrossRef](#)]
44. Ghorbani, M.; Biparva, P.; Hosseinzadeh, S. Effect of colloidal silica nanoparticles extracted from agricultural waste on physical, mechanical and antifungal properties of wood polymer composite. *Eur. J. Wood Prod.* **2018**, *76*, 749–757. [[CrossRef](#)]
45. Yuan, C.; Lin, H.; Lu, H.; Xing, E.; Zhang, Y.; Xie, B. Synthesis of hierarchically porous MnO₂/rice husks derived carbon composite as high-performance electrode material for supercapacitors. *Appl. Energy* **2016**, *178*, 260–268. [[CrossRef](#)]
46. Mathur, L.; Hossain, S.K.S.; Majhi, M.R.; Roy, P.K. Synthesis of nano-crystalline forsterite (Mg₂SiO₄) powder from biomass rice husk silica by solid-state route. *Bol. Soc. Esp. Ceram. V* **2018**, *57*, 112–118. [[CrossRef](#)]
47. Lim, J.L.G.; Raman, S.N.; Lai, F.C.; Zain, M.F.M.; Hamid, R. Synthesis of nano cementitious additives from agricultural wastes for the production of sustainable concrete. *J. Clean Prod.* **2018**, *171*, 1150–1160. [[CrossRef](#)]

Disclaimer/Publisher's Note: The statements, opinions and data contained in all publications are solely those of the individual author(s) and contributor(s) and not of MDPI and/or the editor(s). MDPI and/or the editor(s) disclaim responsibility for any injury to people or property resulting from any ideas, methods, instructions or products referred to in the content.